ISSN 1392 - 1207. MECHANIKA. 2008. Nr.2(70)

Modeling very early age concrete under uniaxial short-time and sustained loading

P. Štemberk*, P. Kalafutová**
**Czech Technical University, Thákurova 7, 16629 Prague 6, Czech Republic, E-mail: stemberk@fsv.cvut.cz*
***Czech Technical University, Thákurova 7, 16629 Prague 6, Czech Republic, E-mail: kalafutova@fsv.cvut.cz*

1. Introduction

Construction of concrete structures using in-situ placement of concrete inherently suffers from the necessity to provide a technological pause for concrete to gain prescribed strength, which eventually slows down the entire construction process. In case of falling behind schedule, construction companies often seek possibilities how to accelerate the construction, which may result in overloading of concrete at extremely early ages. For concrete placed in a well-sealed vertical formwork, the overloading can provide perfect compaction, which is a positive result. But, overloading of newly cast concrete slabs can result in permanent deformation in the form of tracks left by vehicle tires, which in the case of a concrete bridge deck eventually reduces durability of the road surface, which is not allowed to deform uniformly with temperature differences due to the shear locks represented by the imprinted tracks in the surface of the bridge deck.

Premature loading of concrete can be analyzed using a variety of numerical tools, which were created for investigation of early age defects, e.g. [1-3]. Such material models need to take into account the rapidly progressing hydration of concrete. This effect is in most models included as a parameter which expresses the age of concrete in the form of e.g. the degree of hydration or equivalent age. The multilevel models, such as the one presented in [4], do not include the evolution of microstructure as a simple formula, but they use another analysis, where the kinetics of hydration reaction is evaluated on a representative volume.

As the material models are usually derived theoretically, they need to be calibrated and verified with experimental data. The material models then should be also derived with this fact on mind. Usually, the practicing engineers do not have all necessary experimental data at hand which would make the provided material models reliable for their specific applications. This fact was the objective of this paper which provides a simple framework for derivation of a model for expressing mechanical response of concrete subjected to uniaxal short-time and sustained loading at the age of just few hours. The number of material parameters, which can be calibrated with experimental data commonly provided by concrete producing plants, is reduced to minimum, yet with respect to accuracy of the model.

2. Need for modeling of early age concrete

The Border Bridge is a part of the newly constructed D8 highway connecting Prague, CZ, and Dresden, DE. The bridge is located exactly at the border; a part of it is in Germany and the other part is in the Czech Republic. Fig. 1 shows the bridge when it was under construction.

Fig. 1 Border Bridge on D8 highway

This composite bridge is 430 meters long and overpasses a deep valley. The elevation of the bridge is shown in Fig. 2. The maximum height of the bridge measured from the bottom of the valley to the bridge deck is 56.37 meters, which prohibits pumping concrete directly from the bottom of the valley to the reinforced concrete bridge deck. Therefore, the motivation came from the need to transport concrete to the location of placement from the already finished section of the reinforced concrete deck, that means, by placing concrete pumps on newly cast section of the bridge deck.

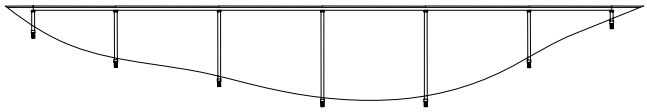

Fig. 2 Longitudinal profile of Border Bridge

3. Proposed modeling

In general, the deformational behavior of concrete at the ages of just a few hours resembles that of already hardened concrete with the distinction of the pronounced plastic deformability which is prominent at the ages between the initial and final setting times. With further increase of age, the ratio between the irreversible and the reversible deformations decreases, which means, the deformation can be distinguished according to its nature. For that reason, the total strain can be split into four components

$$\varepsilon(t)=\varepsilon^{e}(t)+\varepsilon^{v}(t)+\varepsilon^{f}(t)+\varepsilon^{0}(t) \tag{1}$$

where ε^{e} is the elastic or instantaneous strain, ε^{v} is the

reversible viscous strain, ε^f is the irreversible viscous (flow) strain, and ε^0 is the stress-independent strain produced by the hydration process such as autogeneous shrinkage, cracking strain and the thermal strain. The difference between the deformational behavior of hardening concrete and the already hardened concrete is in the pronounced variation in magnitudes of the strain components. At the ages ranging from the time of mixing until about the initial setting time the irreversible viscous strain component ε^f prevails. With progressing hydration the elastic component ε^e and the reversible viscous component ε^v are more pronounced while the prevalence of the irreversible viscous strain component ε^f recedes. The strain component related to the hydration process and stress-independent influences ε^0 is of varying importance throughout the solidification process, which is attributed to the increase of tensile strength of concrete.

The main difference between the hardening concrete and the already hardened one, especially noticeable at sustained loading, is the significant change in the material parameters due to the hydration process which no longer allows the simplifying assumption that material parameters are constant during the whole length of loading. It also should be pointed out that in the case of hardened concrete which is loaded at higher ages the duration of sustained loading can be, and usually is, measured as the time elapsed from the instant of loading until the moment of interest, which is in accordance with the assumption of the constant material parameters. In the case of hardening concrete, duration of sustained loading is actually prescribed in terms of time, however, for modeling it is more convenient to express the duration of sustained loading in terms of the degree of hydration, proposed above, allowing more general considerations which cannot be expressed as a mere time duration. This is, for instance, the effect of elevated temperature due to hydration which further accelerates hydration process and which results in relative contraction of the loading period. Therefore, for the uniaxial response to uniaxial loading the strain should be expressed by

$$\varepsilon(t) = \int_0^t J(h,h')\,d\sigma(t') \tag{2}$$

where J is the compliance function h can be the degree of hydration at the moment of interest t and h' are the degree of hydration at the instant of loading t' ε is strain and σ is stress. The compliance function J is a function of the internal variable, the degree of hydration, on the level of the definition of the model, however, on outside the compliance function J is a function of time. This is consistent since there is a one-to-one mapping between the internal variable and time for given conditions. The strain ε in Eq. (2), represents the sum of the first three components in Eq. (1), excluding the strain component ε^0.

Eq. (1) can be rewritten as a rate-type relation

$$\dot{\varepsilon}(t) = \dot{\varepsilon}^e(t) + \dot{\varepsilon}^v(t) + \dot{\varepsilon}^f(t) + \dot{\varepsilon}^0(t) \tag{3}$$

where the meaning of all entries is identical with those in Eq. (1) and the superposed dot indicates the differentiation with respect to time. The exact definition of each component is given in the following sections.

As this study was focused on the period from the initial setting time up to the final setting time, the effects related to the hydration process, such as autogeneous shrinkage and crack evolution, same as the thermal strain, were not measurable and thus they could not be evaluated. Therefore, at present, the formulation of the strain component ε^0 is not available due to difficulties with obtaining relevant experimental data and so these effects are covered in the other strain components.

3.1. Instantaneous response

The instantaneous deformation of hardening concrete comprises the strain of solid particles of sand and aggregate, the strain of water and the strain of the already hardened cement paste and the not yet hydrated cement grains. These particles can be considered to be nonaging constituents of concrete, which is consistent from the physico-chemical point of view once the effect of aging is dealt with separately.

The aging can be defined as a variation of proportions among the constituents or a ratio between an instant value of a quantity and the value of the quantity when the hydration is completed, which is known as the degree of hydration. Then, the instantaneous response can be represented by the elastic strain rate in the following manner

$$\dot{\varepsilon}^e(t) = \frac{F_e\left[\dot{\varepsilon}(t)\right]\dot{\sigma}(t)}{E(t)} \tag{4}$$

where $E(t)$ is the instantaneous modulus of elasticity and $F_e[\dot{\varepsilon}(t)]$ is a function which expresses the effect of loading rate. The instantaneous modulus of elasticity $E(t)$ can be assumed to be proportional to the microstructural evolution which is expressed in general by the degree of hydration.

3.2. Time-dependent response

The reversible viscous strain represents the strain component which later for the hardened concrete becomes the strain usually described as the viscoelastic. For the sake of consistency of the description of the deformation for both the hardening and hardened concrete the reversible viscous strain component is used for description of the deformation of the hardening concrete, especially the time-dependent, which in its nature resembles that of the already hardened concrete. Even though the term reversible is used as the name of this strain component, in the case of the solidifying and hardening concrete the reversible part of the deformation is negligible when compared with the irreversible part. This reasoning is justified by the experimental data obtained by the author and also by the method of the description of creep of concrete at the very early ages (2 to 7 hours) adopted by Okamoto in [5]. In his work, Okamoto used the viscoelastic three- and four-element rheological models without any clear explanation about the possible reversibility of the creep strain. This may have been for the reason that there were no experimental data on cyclic loading available at that time.

The reversible viscous strain rate can be expressed as follows

$$\dot{\varepsilon}^{v}(t)=\frac{F_v\left[\sigma(t)\right]}{\alpha f_c(t')}\int_0^t \dot{J}^{v}(t,t')d\sigma(t') \tag{5}$$

where $J^{v}(t,t') = J^{v}(t-t')$ is the creep function related to the reversible viscous strain component and it is considered to be a function of the elapsed time during the period when load is applied, which means $J^{v}(t,t')$ is a nonaging material parameter independent of age. The effect of the progressing hydration, which controls the evolution of the microstructure of the hardening concrete, is prominent at the age when concrete solidifies and further hardens and it needs to be included in the modeling. This effect can be expressed directly by a function related to the reversible viscous strain and multiplied by an empirical constant α as seen in the denominator preceding the integral in equation (5). Here, the function is the evolution of compressive strength f_c as this parameter can be obtained very easily. The effect of higher stresses is known to cause an increase in strain rate which is evidenced as the nonlinear deformational behavior. This effect can be included in the description of the reversible viscous strain as a non-dimensional parameter which is a function of the instant stress level at the moment of loading. The effects of a higher stress level is expressed by $F_v[\sigma(t)]$ in the numerator preceding the integral in equation (5).

4. Calibration of model parameters

The uniaxial compression test is probably the far most popular testing method in concrete engineering and so the typical shape of the stress-strain curve of the already hardened concrete subjected to short-time loading is well-known and described, e.g. [6]. The shape of the stress-strain curve obtained on the yet hardening concrete at the ages before the final setting time is similar to that of the already hardened concrete, as can be seen in Fig. 3.

In the proposed modeling, the behavior of hardening concrete subjected to loading conditions defined by the uniaxial compression test configuration is modeled by the sum of elastic response and the time-dependent response, which corresponds with the general formulation in Eq. (1).

The experimental data obtained from the uniaxial compression test, shown in Fig. 3, revealed some similarity with the experimental data acquired from the uniaxial compression test performed with already hardened concrete, where the breaking point, or elasticity limit, in the stress-strain curve is also present. It indicates the yield which takes place at certain yield stress, which is equal to about 40 to 50% of the compressive strength at given age. In order to remain within the elastic region, and thus within the scope of this work, the load level at which the load was kept constant during experiments was set as 30% of the compressive strength at given age. Under these loading conditions, the instantaneous response of the hardening concrete can be expressed with the mere modulus of elasticity, and with the measured Poisson's ratio [7] in case of a multi-dimensional analysis.

Generally, the evolution of concrete strength is faster than the evolution of stiffness. However, based on the quality of the data measured, the evolution of modulus of elasticity is given by

$$E(t)=0.93\,exp(0.7t) \tag{6}$$

where t is age of concrete in hours and which is proportional to the function of the evolution of compressive strength given by

$$f_c(t)=0.01\,exp(0.7t) \tag{7}$$

where t is age of concrete in hours. Eqs. (6) and (7) were obtained by regression analysis of the experimental data for evolution of the modulus of elasticity and the compressive strength, respectively. Comparison of the uniaxial elastic response of concrete calculated with Eq. (4) and the measured data is shown in Fig. 3, where the computed response is indicated by the solid thick lines.

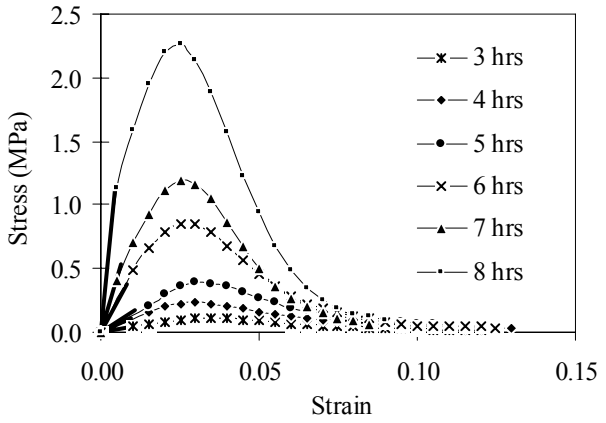

Fig. 3 Comparison of computed and measured short-time elastic response

The response of hardening concrete subjected to sustained uniaxial compression loading is dominated by the irreversible viscous deformation. Development of the creep strain resembles in an accelerated form the creep of the already hardened concrete and the shape resembles especially the so-called viscoelastic part of the strain. However, in the case of hardening concrete, the strain is mostly irreversible which was observed in the experimental data for the short-time cyclic loading under uniaxial loading [3]. Even though the experiment of the reversible creep was not conducted, it is assumed that the time-dependent strain of the hardening concrete under sustained loading is also irreversibly viscous, nevertheless, it is described by the reversible viscous component of the general model. This is for the sake of consistency when it is safe to assume that this part of the strain will later become the reversible viscous strain, known as the viscoelastic strain.

The creep function $J^{v}(t, t')$ which was introduced in Eq. (5), was identified from the experimental data as

$$J^{v}(t-t')=\frac{(t-t')^{\gamma}}{t_0+(t-t')^{\gamma}} \tag{8}$$

where t is time, sec, t' is the instant when the load was applied (in sec) and γ and t_0 are material constants.

The two parameters which are also introduced in Eq. (5) are the scaling parameter α and the function F_v which expresses the effect of load level. Since the relation between evolution of creep strain and evolution of compressive strength was found inversely proportional, the scaling parameter α was considered constant. Because the

cubic concrete specimens were subjected to only one load level of 30% (related to compressive strength at the instant of loading) the effect of load level cannot be expressed here and thus the function F_v is taken as unity. Eq (5) in the absolute-value form, when all parameters related to the concrete considered in the following application are added, becomes

$$\varepsilon^v(t) = \frac{1}{5{,}9\,exp(0.7t')} \int_0^t \frac{(t-t')^{0.95}}{34+(t-t')^{0.95}} d\sigma(t') \qquad (9)$$

Comparison between creep strain calculated with Eq. (9) and measured on cubic specimens at the load level of 30% of compressive strength at the instant of loading is shown in Fig. 4. The comparison proves applicability of the proposed model as it can fit the shape and the magnitude of the measured creep strain satisfactorily.

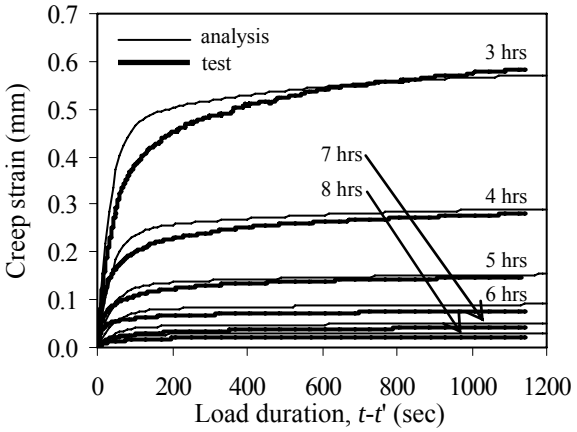

Fig. 4 Comparison of computed and measured time-dependent response

5. Application

5.1. Description of analysis

The formulae for modeling short-time and time-dependent response of hardening concrete at the ages from 3 to 8 hours, which were obtained by fitting the formulae proposed in Section 3 to results shown in Section 4, were used in modeling of a concrete slab subjected to sustained loading by a tire. These were the formulae in Eqs. (4) to (9), which were implemented as such to the finite element code SIFEL, which was done by Dr. Jaroslav Kruis. This code was also successfully used for investigation of another bridge under construction, which is described in [8]. SIFEL - Simple Finite Elements is a finite element code for solving mechanical, transport and coupled problems. SIFEL is free software released under GNU General Public License (GPL). The basic modules of SIFEL are GEFEL (general finite element tools), MEFEL (finite elements for mechanics), TRFEL (finite elements for transport problems), METR (finite elements for coupled problems), PARGEF (parallel version for general finite element tools), PARMEF (parallel version of finite elements for mechanics), PARTRF (parallel version of finite elements for transport problems), PARMETR (parallel version of finite elements for transport problems). The output types of a program created in SIFEL can be text, graphical (GiD, OpenDx, FEMCAD), graphs or tables.

Originally, the concrete bridge deck of the Border Bridge (described in Section 2), shown in Fig. 5, was considered. However, in order to reduce the amount of concrete used in experimental work, the volume of concrete subjected to sustained loading under a tire was defined by a smaller form, whose height as only 100 mm, in contrast to the bridge deck height of 300 mm. Nevertheless, the resulting data can give some clue on the behavior of the concrete bridge deck when loaded prematurely.

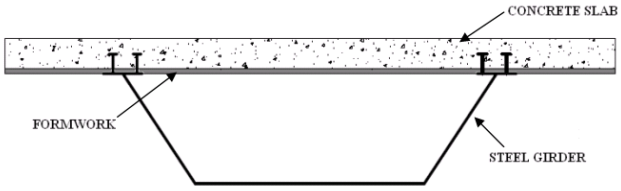

Fig. 5 Cross-section of the bridge deck

The volume of concrete inside the form was converted into a finite element mesh, which is shown in Fig. 6. The size of the elements was 5 x 5 x 2 cm. The load of 45 kN was distributed over an area of 15 x 20 cm, which represents the area of imprint of a cut tire (Fig. 7) used in

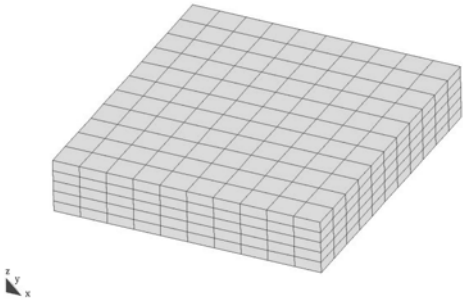

Fig. 6 Three-dimensional model of concrete section under tire

Fig. 7 Pressing cut tire into concrete slab

the experiments. Therefore, the applied compressive stress was always 1.5 MPa, with a small variation caused by the size of the imprint. This variation was considered when processing the data. However, this variation represented an error of up to 10 % in the applied stress.

The concrete used in the experimental work corresponded with the concrete used for the Border Bridge. It was concrete C35/45 with rapid hardening portland cement I 42.5 R. The mix proportions were: water 180 kg/m^3, cement 430 kg/m^3, sand 780 kg/m^3, fine aggregate 140 kg/m^3, coarse aggregate 965 kg/m^3.

5.2. Results of analysis and discussion

The total computed strain of the concrete slab under a truck tire was divided into the instantaneous strain and the time-dependent strain.

The computed instantaneous strain differed from the measured instantaneous strain by 8 to 50%. The error increased with age. This can be attributed to the absolute error in measurements caused by the used strain gauges, which becomes pronounced when concrete is stiffer and thus shows less strain. Therefore, the error may be considered acceptable. The comparison of the computed instantaneous strain and the measured instantaneous strain is given in Table 1.

Table 1

Comparison of computed and measured instantaneous strain

Age (hrs)	Instantaneous strain, mm	
	Computed	Experiment
3	13.39	15.79
4	8.21	8.83
5	5.68	8.30
6	3.41	5.13
7	1.93	2.98
8	1.19	1.78

Comparison between the calculated and measured time-dependent, or creep, strain is shown in Fig. 8. The calculated time-dependent, or creep, strain, shown in Fig. 8, was 2.5 to 5 times higher than the measured one in the experiment. This is in contradiction with the predicted outcome. It was expected that the calculated strain would be lower due to the not included effect of load level which was much higher than the load level considered in derivation of the creep function from the uniaxial compression test. The load level considered in derivation of the model was 30% of the compressive strength at the instant of loading. It should be noted that load levels above about 70% are very difficult to measure in experiments with the standard compressive strength test configuration as the specimen at such early ages begins to disintegrate. On the other hand, load levels about unity can be easily obtained with constrained concrete volumes, which was the case in our experiments with pressing a tire in the concrete slab.

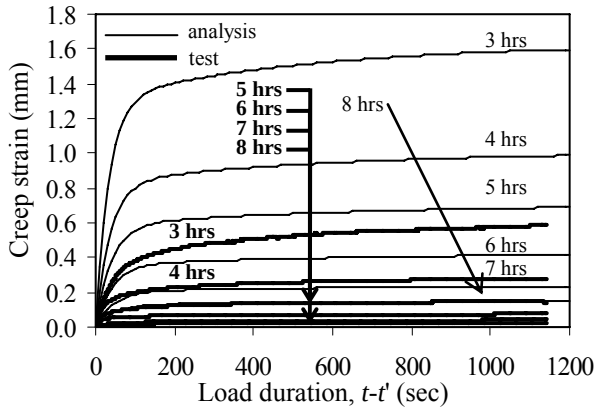

Fig. 8 Comparison of computed and measured time-dependent strain under the tire

Another cause of the difference comes from the rather small depth of the form used, which was only 10 cm. This means that the concrete under the concentrated load may become well-compacted and with the combined effect of the increased friction between concrete and the bottom of the form and the constraint caused by the stiff sides of the form the measured time-dependent strain would be smaller that strain obtained with deeper forms.

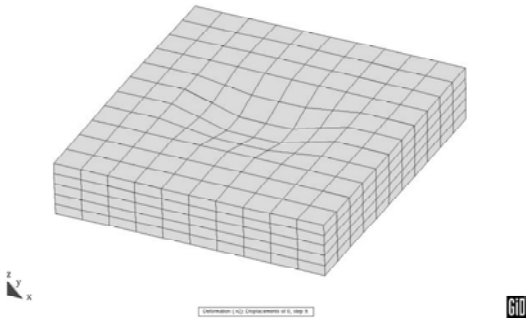

Fig. 9 Example of computed strain of concrete slab under tire

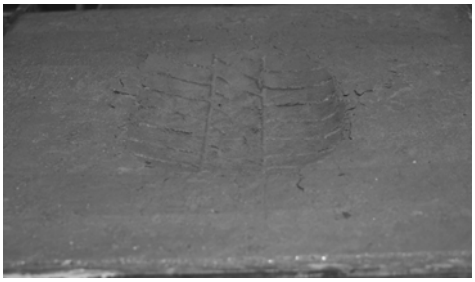

Fig. 10 Image of deformed concrete slab under tire

Also, the effect of the Poisson's ratio should not be neglected. In this analysis, the value was set as 0.35, which corresponds to the value reached in [7, 9] at the load level of 50%. However, as was shown in [7], the apparent Poisson's ratio reaches the value of 0.5 already at the load level of 80%, which was exceeded at all ages in the experiments with the tire pressed in the concrete slab. That means the Poisson's ratio should be considered higher than 0.35, which would pronounce the constraining effect of the stiff form and thus yield lower calculated creep strain. Nevertheless, it should be noted that the computed results are on the safe side. The computed strain and an image of the deformed slab are shown in Figs. 9 and 10, respectively.

6. Conclusions

Based on the experimental data on short-time and time-dependent response of cube specimens obtained with the standard compressive strength test setup, a simple prescription for evolution of modulus of elasticity and compressive strength were derived along with a formula for the creep function, which also takes into account the effect of progressing hydration. These formulas were taken and implemented in the finite element code SIFEL and used for numerical simulation of the test with pressing a cut tire into a concrete slab. The results obtained for instantaneous strain were acceptable with the computed results, when

considering the accuracy of the measuring equipment and configuration. However, the computed creep strain was rather higher than the measured strain.

It was discussed that this may be caused by the size of the form, which at the experiment may have increased friction of the concrete at the bottom of the form and thus reducing the vertical strain. Also, the high load levels may have pronounced the constraining effect of the stiff sides of the form, as the apparent Poisson's ratio at such high load levels may assume the value close to 0.5. Nevertheless, the computed results were 2.5 to 5 times higher than the measured values. Such a result is quite satisfactory when all possible uncertainties related to testing concrete at such early ages are taken into account.

The simplicity of the presented formulas allows an easy calibration with the experimental data commonly provided by concrete producers. Therefore, it can be expected that the formulas would be used by the practicing engineers, especially when the estimations of strain are on the safe side.

Acknowledgement

This work was financially supported by the Czech Science Foundation, projects no. 103/05/2244 and 103/07/1462, which is gratefully acknowledged.

References

1. **Frantová, M.** Modification of Chen model of plasticity for early ages applications.-Mechanika.-Kaunas: Technologija, 2006, Nr.58(2), p.11-16.
2. **Sercombe, J., Hellmich, C., Ulm, F.J., and Mang, H.** Modeling of early-age ereep of shotcrete, I: Model and model parameters.-J. of engineering mechanics, ASCE, 2000, 126(3), p.284-291.
3. **Štemberk, P., Tsubaki, T.** Uniaxial deformational behavior and its modeling of solidifying concrete under short-time and sustained loading.-J. of applied mechanics, JSCE, 2003, 6, p.437-444.
4. **Šmilauer, V., Bittnar, Z.** Microstructure-based micromechanical prediction of elastic properties in hydrating cement paste.-Cement and Concrete Research, 2006, 36(9), p.1708-1718.
5. **Okamoto, H**. A Study on creep properties of concrete at very early age.-Proc. of 30th Japan Congress on Materials Research, 1987, p.171-174.
6. **Židonis, I**. A simple-to-integrate formula of stress as a function of strain in concrete and its description procedure. -Mechanika. -Kaunas: Technologija, 2007, Nr.66(4), p.23-30.
7. **Štemberk, P., Kohoutková, A.** Image-analysis-based measuring of lateral deformation of hardening concrete.-Materials Science (Medžiagotyra), 2005, 11(3), p.292-296.
8. **Brož J., Kruis J.** Modelling of Gradual Construction of Road Bridge and its Creep.-Proc. of Engineering Mechanics 2007 Prague: Institute of Thermomechanics, Academy of Science of Czech Republic, ISBN 978-80-87012-06-2, 2007, p.23-24.
9. **Paulini, P., Gratl, N.** Stiffness Formation of Early Age Concrete, Thermal Cracking in Concrete at Early Ages, edited by R. Springerschmid, E & FN Spon, London, 1994.

P. Štemberk, P. Kalafutová

NESENIAI SUFORMUOTO BETONO VEIKIAMO LINIJINĖS TRUMPALAIKĖS IR ILGALAIKĖS APKROVOS DEFORMACIJŲ MODELIAVIMAS

R e z i u m ė

Straipsnyje pateikiamas modelis, skirtas apskaičiuoti (įvertinti) neseniai suformuoto betono, veikiamo, linijinės trumpalaikės ir ilgalaikės apkrovos, momentinėms ir ilgalaikėms deformacijoms. Pateikiamos visos apskaičiavimams reikalingos formulės ir medžiagos parametrų vertės. Sudarant modelį daugiausia dėmesio buvo skiriama patogiai mažo skaičiaus medžiagos parametrų patikrai su dažniausiai cemento gamintojo pateikiamais eksperimentiniais duomenimis. Siūlomas modelis taikomas kai pradinė ir galinė stingimo ribos kinta nuo 3 iki 8 valandų.

P. Štemberk, P. Kalafutová

MODELLING OF VERY EARLY AGE CONCRETE UNDER UNIAXIAL SHORT-TIME AND SUSTAINED LOADING

S u m m a r y

This paper presents a material model for evaluation of instantaneous and time-dependent strain of concrete subjected to uniaxial short-time and sustained loading at very early ages. All necessary formulas and values of material parameters are given. The emphasis in derivation of the model was put on easy calibration of the small number of material parameters with experimental data commonly provided by concrete producers. The range of applicability of the proposed model is from the initial setting time to final setting time from 3 to 8 hours.

P. Štemberk, P. Kalafutová

МОДЕЛИРОВАНИЕ ДЕФОРМАЦИЙ ТОЛЬКО ЧТО ЗАЛИТОГО БЕТОНА ВОЗДЕЙСТВОВАННОГО ЛИНЕЙНОЙ КРАТКОВРЕМЕННОЙ И ДОЛГОВРЕМЕННОЙ НАГРУЗКОЙ

Р е з ю м е

В статье представлена модель, позволяющая оценить деформацию только что залитого бетона, воздействованного линейной кратковременной и долговременной нагрузкой. Представлены все формулы и значения параметров материала нужные для проведения подсчетов. При создании указанной модели основное внимание было уделено удобной проверке малого числа параметров материала, сравнивая их с экспериментальными данными представленными производителем. Предлагаемая модель может быть использована в диапазоне начальной и конечной границы застывания бетона, продолжающейся от 3 до 8 часов.

Received January 22, 2008

DOI: 10.5755/j02.mech.14949